Resonances in baryon-baryon and pion-deuteron scattering

P. J. Mulders
Los Alamos National Laboratory, Los Alamos, New Mexico 87545
(Received 4 August 1981)

A model to study the influence both of six-quark configurations and of channel coupling in baryon-baryon scattering is presented. In this paper the nonstrange s-wave six-quark (q^6) configurations and channels coupling to them are investigated. The $(I,J^P)=(0,1^+)$ and $(1,0^+)$ q^6 states have a small recoupling to the NN S waves causing repulsion in these waves. The $1,0^+)$ q^6 state couples to πd through quark-antiquark creation and shows up as a resonance in the $^3P_0$ wave. In the $^1D_2$ NN wave a resonant behavior is caused by the NN-$N\Delta$ coupling. The $(1,2^+)$ q^6 state enhances the resonant behavior around the $N\Delta$ threshold. The same enhancements are observed in the $^3P_2$ πd wave. The $(0,3^+)$ q^6 state causes a narrow resonance ($\Gamma\sim 1$ MeV) in the coupled $^3D_3$-$^3G_3$ NN waves.

I. INTRODUCTION

There exists strong experimental evidence for resonancelike behavior in the $^1D_2$ and $^3F_3$ NN waves[1–3] and in some of the πd waves.[4] The coupling of the NN and $N\Delta$ channel can explain a resonancelike behavior.[5] Phenomenological models taking into account coupling of channels show there may be poles in the S matrix.[6,7] The rapid oscillations in the differential cross section for πd (Ref. 4) cannot be explained through coupling to inelastic channels and may be evidence for six-quark states.[8] In this paper we want to incorporate both channel coupling and six-quark states in a model in order to study the influence of both of them in hadron-hadron scattering.

If two baryons are well separated the interactions are described well by potential models[9] which for large and intermediate distances can be theoretically understood.[10,11] At short distances phenomenological contributions such as a hard or soft core need to be introduced. It is not at all surprising that theoretical NN potentials fail to describe the short-range interaction since it is known that hadrons are extended objects with radii of about 1 fm containing a number of quarks. Consequently at short ranges the quark structure of the baryons must be taken into account.

We assume that within a certain radius b the two-baryon system is a six-quark system. If confinement is imposed on this multiquark system, using the MIT bag model, the energies of all possible six-quark states can be calculated and the one-gluon-exchange interaction can easily be taken into account.[12–14] The fact that in a six-quark state the quarks need not be confined to one bag, one attempts to account for by considering multiquark states as poles in a P matrix.[15] The P matrix determines the boundary condition on the scattering wave function at the sphere with radius b. This boundary condition and the long-range interaction determines the wave function at infinity and hence the scattering matrix. For the long-range interaction we use the phenomenological nucleon-nucleon potential. The long-range part (beyond ~ 1 fm) is essentially local and most potentials[9–11] agree with each other quite well. We propose to obtain potentials for the baryon-baryon channels other than NN from a comparison of the quark structure of the NN channel and other baryon-baryon channels. We also obtain the transition potentials between different baryon-baryon channels in this way.

The channels which we investigate in this paper are those NN, $N\Delta$, and $\Delta\Delta$ channels which couple to the simplest six-quark configurations, namely, those where all quarks are in s waves. The six-quark states are denoted $D(I,J^P;M)$; I is the isospin, J^P the spin and parity, and M the mass in GeV. Four such six-quark states coupling to NN channels are possible, $D(0,1^+;2.16)$, $D(1,0^+;2.24)$, $D(1,2^+;2.36)$, and $D(0,3^+;2.36)$. The masses given here are those calculated using the MIT bag model.[12–14] We consider only two-body channels and do not take the width of the Δ baryon into account. We also take the πd channel into account and assume it to be coupled to the $N\Delta$ channel. We calculate the S matrix and discuss its dependence on channel coupling and dibaryon poles in the P matrix. The results are compared with the existing phase-shift analyses for NN scattering.

The paper is organized as follows. A short review of the s-wave six-quark states is given in Sec. II. The connection between six-quark states and the baryon-baryon scattering wave function using the P matrix is explained in Sec. III. The long-range interaction used in the baryon-baryon channels is explained in Sec. IV. The results are discussed in Sec. V. Finally the conclusions are given in Sec. VI.

II. SIX-QUARK STATES

In order to classify the six-quark states (q^6) and to determine their coupling to baryon-baryon ($q^3 \times q^3$) channels, Young diagrams (YD's) are used to label the irreducible representations (irreps) of the symmetry group to which the q^6 wave function or its spatial, color, spin, or isospin part belong. The YD's are denoted by the number of boxes in each row, $[r_1 r_2 \ldots]$. The corresponding irreps of the SU(n) groups are denoted by their dimension N, $\{N\}$ for SU(6), $\underline{N}$ for SU(3), and N for SU(2).

The total q^6 wave function is antisymmetric (YD $[1^6]$). Its spatial part is symmetric when all quarks are in s waves (YD [6]); this uniquely determines the color$\times$spin$\times$isospin part to be represented by the associated YD of the spatial part, namely $[1^6]$. The various spin and isospin configuration for color singlets—we only consider nonstrange quarks (u,d)—are given in Table I.

If only one quark flavor is considered (e.g., u quarks, thus $I=3$) the q^6 state belongs to the (one-dimensional) antisymmetric color$\times$spin SU(6) irrep, cs$=\{1\}$ (YD $[1^6]$); its decomposition into SU(3)$\times$SU(2) irreps only contains a color singlet with spin zero,

$$\{1\} \supset (\underline{1},1)\ .$$

The q^3 system belongs in the case of only u quarks ($I=\frac{3}{2}$) to the antisymmetric color$\times$spin SU(6) irrep, cs$=\{20\}$ (YD $[1^3]$) which contains the color SU(3) and spin SU(2) irreps

$$\{20\} \supset (\underline{1},4)+(\underline{8},2)\ .$$

The coupling of the $I=3$ q^6 state to color-singlet and color-octet $q^3 \times q^3$ state is determined by the isoscalar Clebsch-Gordon coefficients,

$$\left[\begin{array}{c|cc} 1 & 20 & 20 \\ \underline{1},1 & \underline{1},4 & \underline{1},4 \end{array}\right] = \left[\begin{array}{c|cc} [1^6] & [1^3] & [1^3] \\ [2^3],[3^2] & [1^3],[3] & [1^3],[3] \end{array}\right] = \left(\tfrac{1}{5}\right)^{1/2}$$

and

$$\left[\begin{array}{c|cc} 1 & 20 & 20 \\ \underline{1},1 & \underline{8},2 & \underline{8},2 \end{array}\right] = \left[\begin{array}{c|cc} [1^6] & [1^3] & [1^3] \\ [2^3],[3^2] & [21],[21] & [21],[21] \end{array}\right] = \left(\tfrac{4}{5}\right)^{1/2} .$$

The recoupling to baryon-baryon channels is also given in Table I. If more than one quark flavor is considered there is more than one color-singlet and color-octet channel.[16] Taking together all flavor and spin possibilities for color-singlet and color-octet channels respectively the isocalar coefficients are identical to the ones given above, with spin irreps replaced by flavor$\times$spin irreps; the sum over the squares of the recoupling coefficients thus remains $\frac{1}{5}$ for the color-singlet and $\frac{4}{5}$ for the color-octet channels. The color-octet channels are not specified in Table I; only the isoscalar coefficients to all color-octet channels (B_8B_8) is given. Note that in $q^3 \times q^3$ (color$\times$ spin$\times$flavor $[1^3]\times[1^3]$) more configurations are possible than just the one with YD $[1^6]$. If all quarks are in s

TABLE I. Dibaryons (s-wave q^6 states) and their recoupling to baryon-baryon channels; I=isospin; J^P=spin-parity; M=mass in GeV calculated using the MIT bag model.

$D(I,J^P;M)$	Recoupling
$D(0,1^+;2.16)$	$(\frac{1}{9})^{1/2}NN+(\frac{4}{45})^{1/2}\Delta\Delta+(\frac{4}{5})^{1/2}B_8B_8$
$D(1,0^+;2.24)$	$(\frac{1}{9})^{1/2}NN+(\frac{4}{45})^{1/2}\Delta\Delta+(\frac{4}{5})^{1/2}B_8B_8$
$D(1,2^+;2.36)$	$(\frac{1}{6})^{1/2}N\Delta+(\frac{1}{30})^{1/2}\Delta\Delta+(\frac{4}{5})^{1/2}B_8B_8$
$D(0,3^+;2.36)$	$(\frac{1}{5})^{1/2}\Delta\Delta+(\frac{4}{5})^{1/2}B_8B_8$
$D(2,1^+;2.51)$	$-(\frac{1}{6})^{1/2}N\Delta-(\frac{1}{30})^{1/2}\Delta\Delta+(\frac{4}{5})^{1/2}B_8B_8$
$D(3,0^+;2.83)$	$(\frac{1}{5})^{1/2}\Delta\Delta+(\frac{4}{5})^{1/2}B_8B_8$

waves, however, this configuration is the only one allowed by the Pauli principle. For excited quark states also other configurations occur.[17]

III. CONTRIBUTION OF SIX-QUARK STATES

The connection between q^6 states and the scattering of two baryons ($q^3 \times q^3$) is established through the P matrix.[15]

The P matrix is determined by the logarithmic derivative of the scattering wave function at some radius b. For the radial wave function in a single s-wave channel when there is no interaction for $r > b$ it is

$$\frac{b(du/dr)_b}{u(b)} = P = kb\cot(kb+\delta) . \tag{1}$$

The P matrix has poles at those energies for which the wave function vanishes at b. This is illustrated in the P matrix in the absence of interaction using the expansion for $x\cot x$. In an S-wave channel (labeled α) the free P matrix is

$$\frac{b(du_\alpha/dr)_b}{u_\alpha(b)} = P^{(0)}_{\alpha\alpha} = k_\alpha b\cot k_\alpha b = 1 + \sum_{n=1}^{\infty} \frac{2k_\alpha{}^2}{k_\alpha{}^2 - n^2(\pi/b)^2} . \tag{2}$$

It is assumed that a spherical (s-wave) q^6 bag state with bag radius R_{bag} corresponds to a pole of P in the corresponding S-wave $q^3 \times q^3$ channels. In Ref. 15 it is argued that b is related to the bag radius which works reasonably well in low-energy meson-meson and baryon-meson scattering. In baryon-baryon scattering we would have $b = 1.14 R_{\text{bag}}$; an important part of the interaction, however, is the long-range interaction between two bags; since there is still little known about the mechanism of two bags merging into one bag,[18] we consider the transition radius b in baryon-baryon scattering as a free parameter. The P matrix for S-wave baryon-baryon channels we take to be the free matrix $P^{(0)}$ (Eq. 2) in which only the position and residues of the lowest poles are modified[19]; these poles correspond to solutions which have their first node at $r = b$. The position is put at the energy of the bag-model q^6 state. A more difficult point is what to do with the residues. An estimate using the bag model first of all would require the contruction of proper momentum eigenstates. We make the following assumptions for the residue: we single out the factors for the recoupling of q^6 to $q^3 \times q^3$ states, as given in Table I. The residue is found by multiplying these factors with $2k_i{}^2$; here k_i is an effective momentum which for s-wave states equals (π/b) at the position of the pole.[20] With this choice for the residue the free P matrix is recovered when the recoupling factor equals one and the bag state has the same energy as the lowest pole in the free P matrix; one can see this as turning off all interactions in which case it does not matter whether we consider the system as $q^3 \times q^3$ or q^6. In formula, the P matrix for the S-wave baryon-baryon channels including q^6 states (labeled i, energy $\sqrt{s_i}$) is

$$P_{\alpha\beta} = \left[k_\alpha b\cot k_\alpha b - \frac{2k_\alpha{}^2}{k_\alpha{}^2 - (\pi/b)^2} \right] \delta_{\alpha\beta} + \sum_i \frac{2k_i^2 \lambda_\alpha^{(i)} \lambda_\beta^{(i)}}{k_i^2 - (\pi/b)^2} , \tag{3}$$

where

$$k_i{}^2 = \tfrac{1}{4}(s - s_i) + (\pi/b)^2 .$$

The $\lambda_\alpha^{(i)}$'s are the recouplings for the ith six-quark state to the baryon-baryon channel α. The P matrix in Eq. (3) has the correct analytic properties and asymptotic behavior. It is real for real energies and has simple poles at the real axis. It has no two-body threshold singularities.[21] An important advantage of using the P matrix is that no angular-momentum-barrier factors are needed in the residues of the poles. The correct threshold behavior is automatically obtained.

The P matrix gives the connection between the q^6 states and $q^3 - q^3$ scattering. It determines the boundary condition for the scattering wave function at b. The scattering wave function u is parametrized by the S matrix.

$$u = \left[\frac{1}{k} \right]^{1/2} (I + OS) , \tag{4}$$

where I and O are the scattering wave functions—in the multichannel case diagonal matrices—which, when no long-range interactions (e.g., Coulomb) are present, satisfy the boundary conditions (L wave)

$$I(k,r) \underset{r\to\infty}{\longrightarrow} krh_L^{(2)}(kr) ,$$

$$O(k,r) \underset{r\to\infty}{\longrightarrow} krh_L^{(1)}(kr) . \tag{5}$$

The relation between the P and the S matrices is given by

$$P = x^{1/2}[I'(x)+O'(x)S] \times [I(x)+O(x)S]^{-1}x^{1/2}\,|_{x=kb} ,$$

which is the generalization of Eq. (1) to arbitrary waves and more channels and which is valid at any radius b.

IV. THE LONG-RANGE INTERACTION

We have assumed that the baryon-baryon system could be described as a six-quark system for baryon-baryon separation less than b. The bag-model calculations for six-quark states can be used to guide us in the choice of poles, their energies, and their residues in the P matrix. Through the P matrix we can get a boundary condition for the scattering wave function at the radius $r=b$. When there is no (long-range) interaction the free scattering wave functions can be used in Eq. (6) to establish the connection between the S and P matrices. Examples are meson-meson scattering[15] and baryon-meson scattering.[22] In the case of baryon-baryon scattering, however, the long-range one-boson-exchange interaction, especially one-pion exchange, is important.[23]

For baryon-baryon separation larger than b we use the following potential between baryons 1 and 2 (at distance $\vec{r}$),

$$V_{12}(r) = \sum_{\substack{i\in 1\\ j\in 2}} V_{ij}(r) , \tag{7}$$

where the sum rules over quarks in baryons 1 and 2. V_{ij} is an effective quark-quark potential depending on the isospin and spin of quarks i and j. These potentials are determined from the phenomenological NN potentials, applying Eq. (7) and considering all spin and isospin combinations of the NN system (see Appendix). As an example the OPE potential between two nucleons is obtained from a similar potential between two quarks,

$$V_{ij} = [\,(\vec{\sigma}_i\cdot\sigma_j)(\vec{\tau}_i\cdot\vec{\tau}_j)V_0(r) + S_{ij}(\vec{\tau}_i\cdot\vec{\tau}_j)V_2(r)] , \tag{8}$$

where

$$S_{ij} = [3(\vec{\sigma}_i\cdot\hat{r})(\vec{\sigma}_j\cdot\hat{r}) - \vec{\sigma}_i\cdot\vec{\sigma}_j] , \tag{8a}$$

$$V_0(r) = \frac{f^2}{4\pi}\frac{m_\pi}{3}\frac{e^{-x}}{x}\bigg|_{x=m_\pi r} , \tag{8b}$$

$$V_2(r) = V_0(r)\left[1+\frac{3}{x}+\frac{3}{x^2}\right]\bigg|_{x=m_\pi r} \tag{8c}$$

(m_π is the pion mass). The coupling constant $f^2/4\pi$ is related to the $NN\pi$ coupling constant by

$$f^2/4\pi = \tfrac{9}{25} f_{NN\pi}{}^2/4\pi . \tag{9}$$

We assume that the baryon-baryon potentials obtained from Eq. (7) can be used in the following relativistic Schrödinger equation for the radial wave function u in the region $r > b$,

$$\left[-\frac{d^2}{dr^2}+\frac{l(l+1)}{r^2}+\tfrac{1}{2}\sqrt{s}\,V - k^2(s)\right]u(r) = 0 , \tag{10}$$

where $\sqrt{s}$ is the c.m. energy, $k^2(s)$ is the relativistic relation between energy and momentum squared, and $(\sqrt{s}/2)V$ is the equal-mass result of $\sqrt{2\mu}V\sqrt{2\mu}$ where $\mu = k/v_{\rm rel}$ ($v_{\rm rel}$ is the relative velocity in the c.m. system). The parametrization of the scattering wave function with the S matrix then is like that in Eq. (4), although this is not the nonrelativistic wave function. Since the potentials are constructed in such a way that in the NN case for low energies the correct phenomenological potentials are found, the results using Eq. (10) will only be different at higher energies ($\sqrt{s} \gtrsim 2.1$ GeV) where the energy dependence in Eq. (10) becomes more important. In the construction of the potentials the mass breaking effects between NN, $N\Delta$, and $\Delta\Delta$ channels have been neglected. For the moment, however, we are mainly interested in the qualitative features in baryon-baryon scattering and we think this approach will give reasonable result.

V. RESULTS

We calculate the scattering matrix for the channels coupling to each one of the dibaryons in Table I if they at least couple to an NN channel. These are the first four entries in Table I; the last two states have no connection to NN or πd channels. In order to compare the influence of channel coupling and dibaryons we compare some of the following cases:

Case I. Only the NN channels are considered with long-range interaction for $r > b$. The P matrix for the free case [Eq. (2)] is used, which means that there is no interaction for $r < b$.

Case II. All possible baryon-baryon (BB) channels NN, $N\Delta$, and $\Delta\Delta$ are considered with interaction for $r > b$ and no interaction for $r < b$.

Case III. BB channels with long-range interaction and πd channel are considered. The πd channel is coupled to $N\Delta$ using a potential which is roughly proportional to the deuteron wave function squared for $r > b > a_1$,

$$V_{\pi d\text{-}N\Delta}(r) = V_0(r - a_1)e^{-r/a_2}, \tag{11}$$

with $V_0 = 20$ MeV, $a_1 = 3$ GeV^{-1}, $a_2 = 6$ GeV^{-1}. There is no interaction for $r < b$.

Case IV. All channels (case III) are considered. In this case the logarithmic derivative in the BB channels is given by the P matrix in Eq. (3); dibaryon poles coupling to the BB channels (only $\lambda_{BB} \neq 0$) are taken into account. There is no interaction in the πd channel for $r < b$.

Case V. In addition to case IV we also add interaction in the πd channel through the P matrix. Dibaryon states can couple to the πd channel through their $q^7\bar{q}$ component, just like the ρ couples to $\pi\pi$ through the $q^2\bar{q}^2$ component. Dibaryon poles coupling to the BB and πd channels (also $\lambda_{\pi d} \neq 0$) are taken into account.

A number of parameters have been used. Most of the qualitative features do not depend on the precise values of the parameters. The parameters and the used values are as follows.

(1) The radius b separating the six-quark and the baryon-baryon domains. A value $b = 5$ GeV^{-1} is used. Due to the angular momentum barrier the results for $L \neq 0$ waves are not very sensitive for the precise value of b. Only for the S waves the phase shifts at low energies ($\sqrt{s} < 2.0$ GeV for NN) are sensitive to the value of b. The value of b, which we use, is required to get sufficient attraction in the NN S waves.

(2) For the energies of the dibaryon poles we use the bag-model values in Table I as a guideline. Whenever the specific choice of the position is important, e.g., with respect to thresholds, we discuss such.

(3) For the residue of the dibaryon poles the values in Table I are used for the BB channels. For the πd channel a residue $\lambda_{\pi d} = 0.15$ is used in case V. Such a value is needed to explain the observed inelasticity in the $^1S_0$ NN wave.

(4) The phenomenological NN potential has been used to determine the effective quark-quark potentials. With Eq. (7) then all BB potentials are calculated. The πd-$N\Delta$ interaction has been discussed above (case III); a different-shaped potential does not affect the qualitative features.

The results for NN waves are given using the following parametrization of the S marix. For uncoupled waves ($L = J$)

$$S = \eta e^{2i\delta}, \tag{12}$$

where $\eta \to 1$ if no inelastic channels contribute; for coupled waves ($L = J \pm 1$)

$$S = \begin{bmatrix} \lambda_-^2\cos 2\epsilon' e^{2i\delta_-} & i\lambda_+\lambda_-\sin 2\epsilon' e^{i(\delta_+ + \delta_-)} \\ i\lambda_+\lambda_-\sin 2\epsilon' e^{i(\delta_+ + \delta_-)} & \lambda_+^{-}\cos 2\epsilon' e^{2i\delta_+} \end{bmatrix} \tag{13}$$

which essentially are the nuclear bar phase shifts with complex angles $\delta_\pm \to \delta_\pm - i\ln\lambda_\pm$, $\epsilon \to \epsilon' + i\phi$.[24] When there are no inelastic channels contributing all angles become real, i.e., $\lambda_\pm \to 1$, $\phi \to 0$. For other channels such as $NN \to \pi d$ or $\pi d \to \pi d$, Argand plots are given.

A. The $D(0,1^+)$ dibaryon

The $(I,J^P) = (0,1^+)$ channels which have been taken into account, the mass M_p of the $D(0,1^+)$ pole, and its coupling to the channels (see Table I) have been given in Table II. For cases I and IV the NN nuclear bar phase shifts have been given in Fig. 1. The coupling of NN and $\Delta\Delta$ channels has barely any influence in the energy region below 2.5 GeV, at least in the NN channels. The dotted line shows the result when the free P matrix [Eq. (2)] is used. The lowest pole then lies at 2.26 GeV ($k_{NN} = \pi/b$) and has a residue $\lambda_{NN} = 1$. Including the $D(0,1^+)$ dibaryon (pole position chosen at 2.24 GeV) causes the repulsion below 2.20 GeV followed by a steep rise in the $^3S_1$ phase shift around the pole position. The repulsion is due to the small residue for the $D(0,1^+)$, $\lambda_{NN}^2 = \frac{1}{9}$. Increasing the residue with a factor 2 (Fig. 1) yields less repulsion and a slightly less steep rise, but it does not give an improvement especially not for the $^3D_1$

TABLE II. Parameters for $(I,J^P) = (0,1^+)$ channels.

α	Channel	Partial wave	λ_α (Table I)
1	NN	$^3S_1$	0.333
2	NN	$^3D_1$	0
3	$\Delta\Delta$	$^3S_1$	0.298

$M_p = 2.24$ GeV

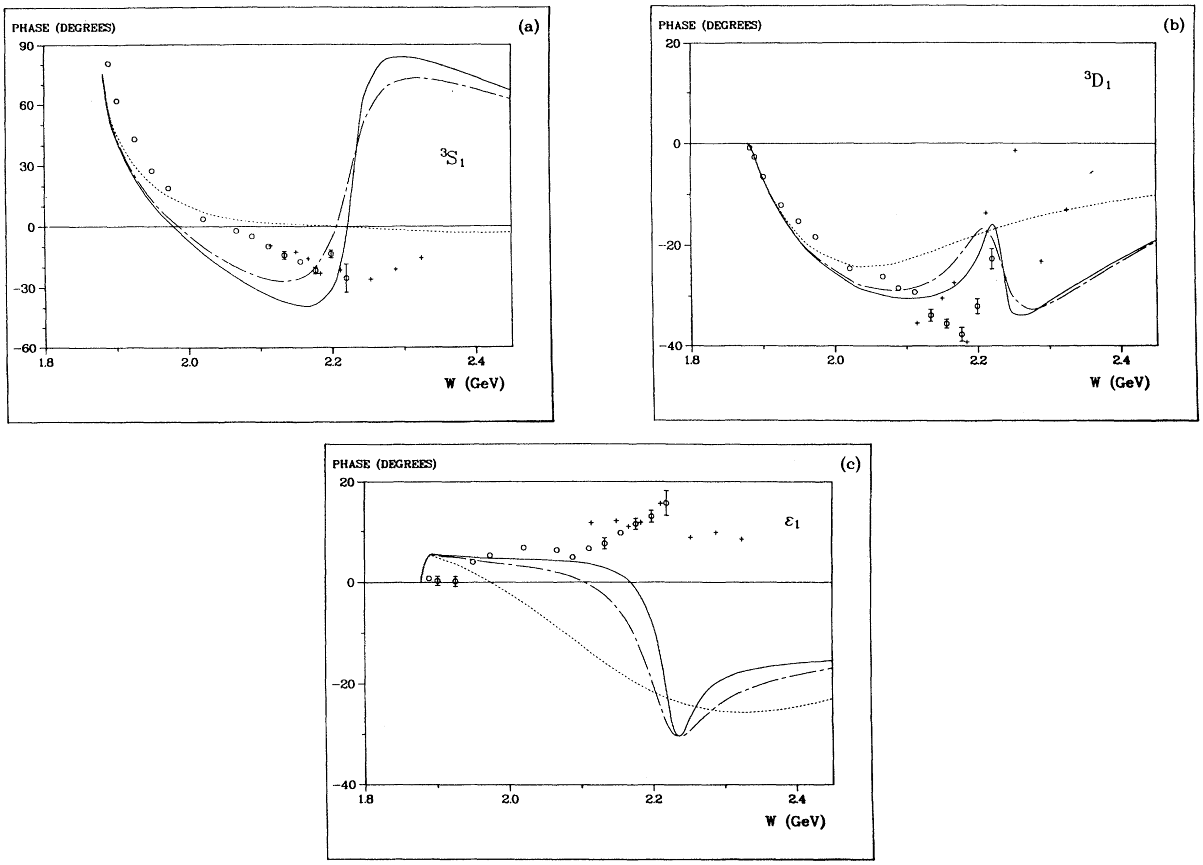

FIG. 1. The (complex) nuclear bar phase shifts for the coupled $^3S_1$-$^3D_1$ NN waves [Eq. (13)]. Below the $\Delta\Delta$ threshold $\lambda(^3S_1)=\lambda(^3D_1)=1$, $\phi_1=0$. Given are (a) $\delta(^3S_1)$, (b) $\delta(^3D_1)$, and (c) ϵ_1 for case I (dashed line) and IV (solid line). The chain-dashed line is the result when the residue is multiplied by a factor 2. The experimental points are from Refs. 1 (circles) and 3 (crosses).

wave. The widths of the effects in $\delta(^3S_1)$, $\delta(^3D_1)$, and ϵ_1 are of the order of 30 MeV. No considerable rise of the phase shift has yet been observed in the $^3S_1$ NN wave up to $\sqrt{s}=2.22$ GeV.[1] In the $^3D_1$ wave, however, the calculated phase shift qualitatively agrees with the experimental phase shift,

TABLE III. Parameters for $(I,J^P)=(1,0^+)$ channels.

α	Channel	Partial wave	λ_α (Table I)
1	NN	$^1S_0$	0.333
2	$N\Delta$	$^5D_0$	0
3	$\Delta\Delta$	$^1S_0$	0.298
4	πd	$^3P_0$	0.15[a]
$M_p=2.28$ GeV			

[a]In case V coupling to the πd channel is assumed.

with the chosen value for the mass of pole. The agreement would have been far worse when the bag model value for the mass would have been used.

We have remarked before that the NN S waves require the value $b=5$ GeV^{-1}. If one would try to fit the scattering lengths in $^3S_1$ and $^1S_0$ waves more accurately, slightly different values for b are needed, e.g., $b=4.95$ GeV^{-1} for the $^3S_1$ wave. This reflects the strong dependence on b for very low energies.

B. The $D(1,0^+)$ dibaryon

The parameters for the $(I,J^P)=(1,0^+)$ channels have been given in Table III. The results for cases IV and V in the NN $^1S_0$ wave have been given in Fig. 2; the results for the $^3P_0$ πd wave in Fig. 3. As for the case of the $(0,1^+)$ channel the dibaryon pole causes the repulsion which is due to the small

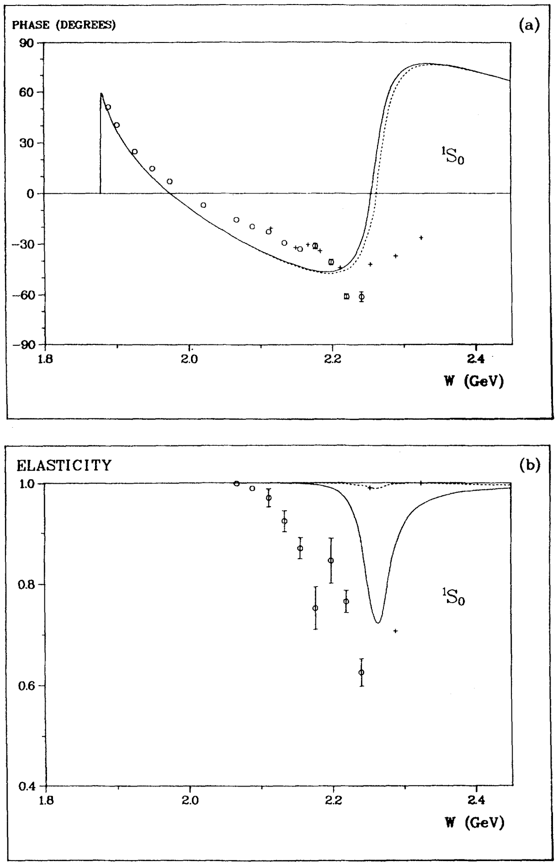

FIG. 2. The phase shift (a) and elasticity (b) for the NN $^1S_0$ wave [Eq. (12)] for cases IV (dashed line), and V (solid line). The experimental points are from Refs. 1 (circles) and 3 (crosses).

residue, $\lambda_{NN}^2=\frac{1}{9}$. Around the pole position (chosen at 2.28 GeV) there is a steep rise in $\delta(^1S_0)$. It is noticeable that we can only get sufficient inelasticity by assuming that the dibaryon state has a coupling to the πd channel (compare cases IV and V); the actual agreement with the experimental phase-shift analyses, however, is only qualitative. In the case a coupling to the πd channel is assumed an inelastic resonance shows up in the $^3P_0$ πd wave between 2.25 and 2.30 GeV (Fig. 3); the width depends on the coupling of the dibaryon to the πd channel, $\Gamma \sim \lambda_{\pi d}^2$.

C. The $D(1,2^+)$ dibaryon

The parameters for the $(I,J^P)=(1,2^+)$ channels have been given in Table IV. The results for the cases I, III, IV, and V have been given in Figs. 4 and 5. The strong coupling of the NN and $N\Delta$ channels through the long-range interaction is sufficient to explain a resonant behavior at the opening of the $N\Delta$ channel (case III). Including a dibaryon pole in the P matrix causes an enhancement

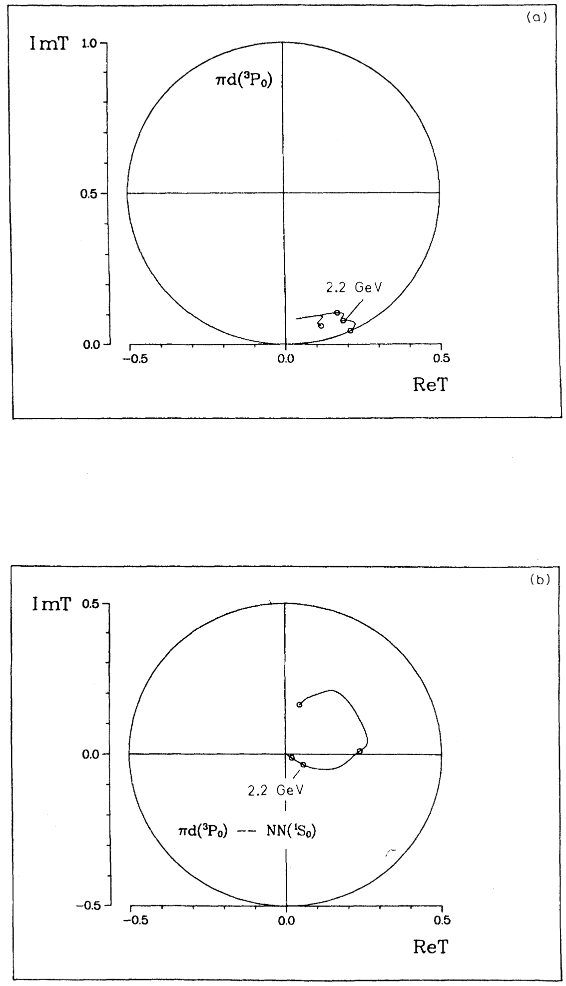

FIG. 3. Argand plots for (a) $\pi d \to \pi d$ and (b) $NN \to \pi d$ T-matrix elements for $(I,J^P)=(1,0^+)$ for case V; the marks are given at every 50 MeV starting from $\sqrt{s}=2.15$ GeV.

TABLE IV. Parameters for $(I,J^P)=(1,2^+)$ channels.

α	Channel	Partial wave	λ_α (Table I)
1	NN	$^1D_2$	0
2	$N\Delta$	$^5S_2$	0.408
3	$\Delta\Delta$	$^5S_2$	-0.183
4	πd	$^3P_2$	0.15[a]
$M_p=2.30$ GeV			

[a]In case V coupling to the πd channel is assumed.

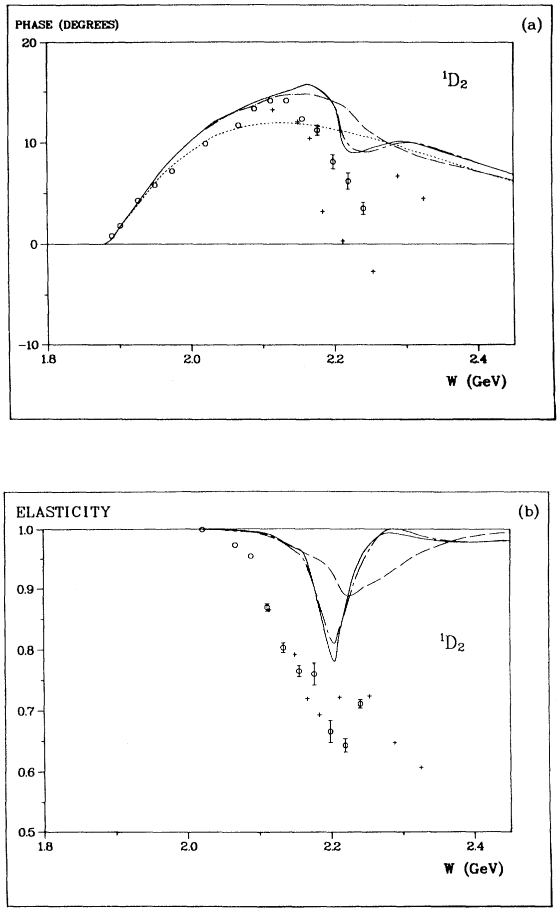

FIG. 4. The phase shift (a) and elasticity (b) for the NN $^1D_2$ wave [Eq. (12)] for cases I (dashed line), III (chain-dotted line), IV (chain-dashed line), and V (solid line). The experimental points are from Refs. 1 (circles) and 3 (crosses).

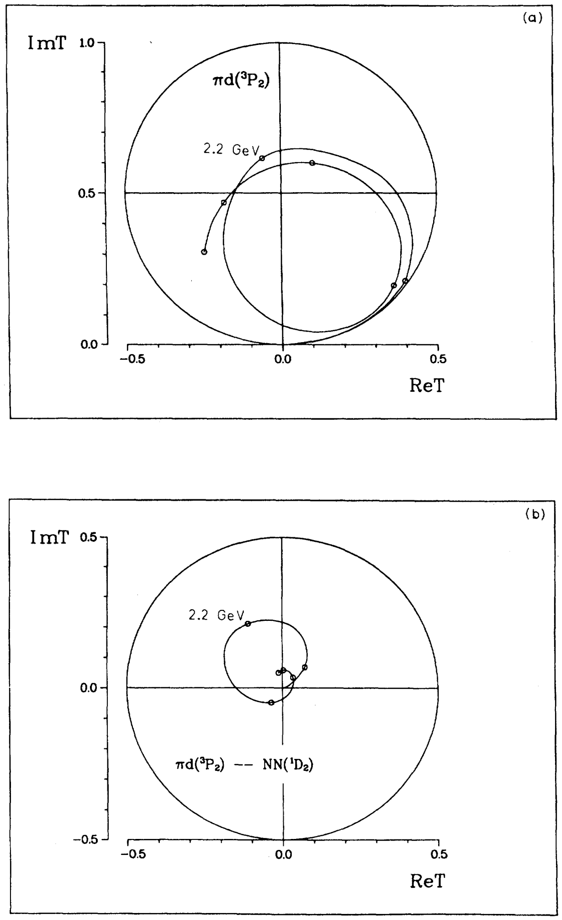

FIG. 5. Argand plots for (a) $\pi d \to \pi d$ and (b) $NN \to \pi d$ T-matrix elements for $(I,J^P)=(1,2^+)$ for cases V; the marks are given at every 50 MeV starting from $\sqrt{s}=2.5$ GeV.

of the resonant behavior, at least when its energy is not too far from the $N\Delta$ threshold. We have chosen 2.30 GeV. The pole has less influence on the NN channel when its energy is higher. When it is considerably lower (<2.2 GeV) the behavior becomes narrower and starts to resemble the case of $(I,J^P)=(0,3^+)$ which will be considered in Sec. V D. Also the πd $^3P_2$ wave shows a resonancelike behavior in cases III–IV, which is reasonably in agreement with the πd phase-shift analysis of Ref. 25. Above 2.2 GeV a second loop in the Argand plot appears in the case V when the dibaryon pole has a nonzero residue to πd, $\lambda_{\pi d}=0.15$. This is shown in Fig. 5. The widths of the resonant behavior in $^1D_2$ NN and $^3P_2$ πd waves is about 50 MeV. We should note that we have not taken into account the width of the Δ.

D. The $D(0,3^+)$ dibaryon

The parameters for the $(I,J^P)=(0,3^+)$ channels have been given in Table V. The results for cases I, II, and IV have been given in Fig. 6. The estimate of the mass of the $D(0,3^+)$ from the bag model indicates that this dibaryon is a $\Delta\Delta$ bound state. Through the coupling of $\Delta\Delta$ and NN channels there exists the possibility of it decaying into the NN $^3D_3$-$^3G_3$ waves. It shows up as a elastic resonance with a small width. If the dibaryon pole position is chosen at 2.30 GeV, the resonance parameters are

$$M_{\rm res} \cong 2.271 \text{ GeV} , \quad \Gamma \cong 1.0 \text{ MeV} .$$

TABLE V. Parameters for $(I,J^P)=(0,3^+)$ channels.

α	Channel	Partial wave	λ_α (Table I)
1	NN	$^3D_3$	0
2	NN	$^3G_3$	0
3	$\Delta\Delta$	$^7S_3$	0.447
$M_p=2.30$ GeV			

VI. DISCUSSION

In order to describe the interaction between two baryons we have chosen a region of space outside which the system is described as a baryon-baryon system and inside which the system is a six-quark system. These choices of basis states, $q^3 \times q^3$ or q^6, are appropriate in view of the interactions, namely, between the baryons at large baryon-baryon distances, and between the quarks at short distances. A phenomenon such as the medium-energy negative phase shift in the NN S waves is a direct consequence of the Pauli exclusion principle in a six-quark system. This is clearly exhibited when six-quark configurations with the same quantum numbers as the NN S waves are taken into account [Figs. 1(a) and 2(a)]. The small coupling to color-singlet baryon-baryon waves ($\frac{1}{5}$) has the effect of a core. The sharp rise around the pole positions is also an effect caused by the small residue (Fig. 1). The S waves are rather sensitive to the choice of the transition radius b. For the $L \neq 0$ waves the results do not depend strongly on the transition region; this region is made less important by the angular momentum barrier.

The results in the $^1D_2$ NN wave shows that the

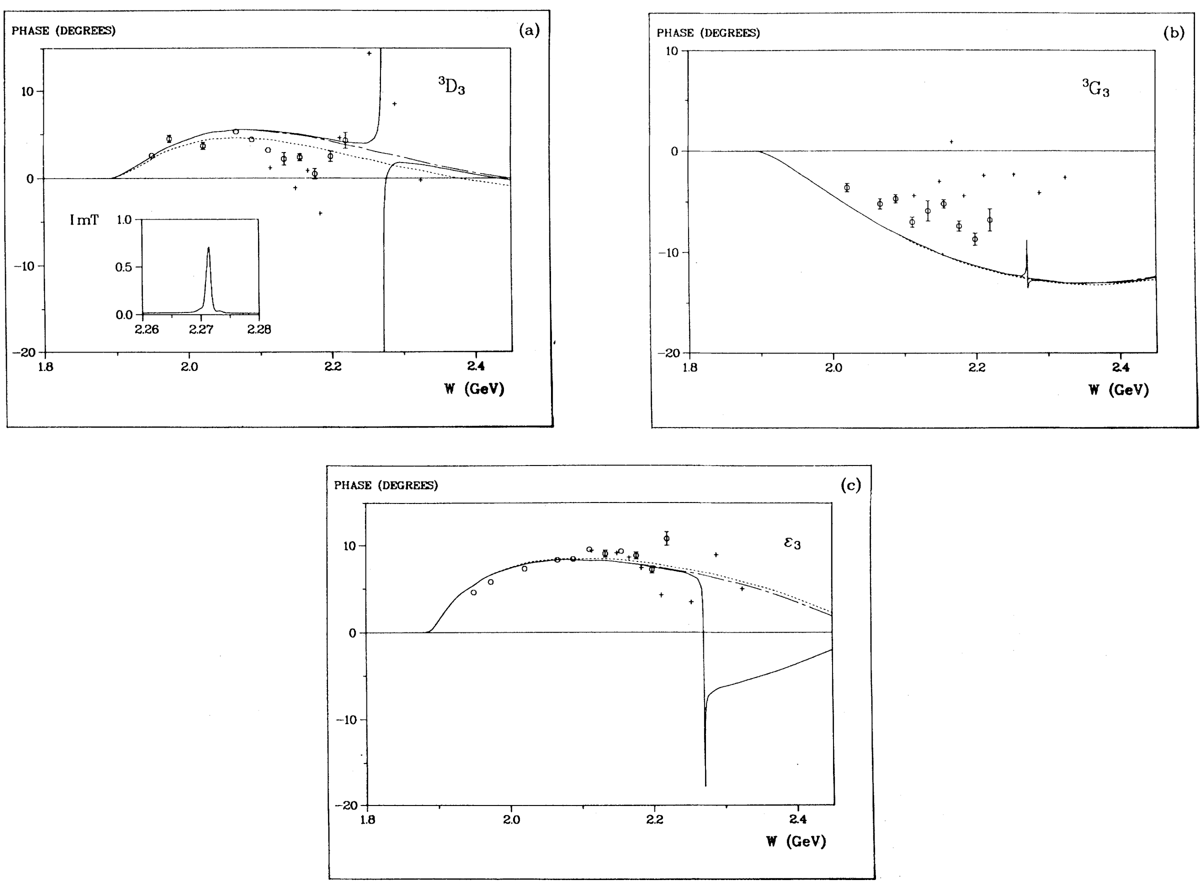

FIG. 6. The (complex) nuclear bar phase shifts for the coupled $^3D_3$-$^3G_3$ NN waves [Eq. (13)]. Below the $\Delta\Delta$ threshold $\lambda(^3D_3)=\lambda(^3G_3)=1$, $\phi_3=0$. Given are (a) $\delta(^3D_3)$, (b) $\delta(^3G_3)$, and (c) ϵ_3 for cases I (dashed line), II (chain-dashed line), and IV (solid line). The experimental points are from Ref. 1 (circles) and 3 (crosses). The inset shows ImT for the NN $^3D_3$ wave near the resonance in case IV.

coupling of channels has a large influence and obscures nearby six-quark dibaryons. The channel coupling by itself already causes a resonant behavior. In the $^1D_2$ NN wave—and also the $^3F_3$ NN wave[26]—the NN-$N\Delta$ coupling causes the behavior around or just above the $N\Delta$ threshold, not only in the NN wave but also in the corresponding πd wave. The width of this kind of resonances is, as one can expect, of the order 50–100 MeV. The widths of resonances due to six-quark states, however, might cause rather narrow effect as we have found in $^3D_1$ NN, $^3P_0$ πd, and $^3D_3$ NN waves.

The general agreement with the data is best for low energies. This is an obvious result since we use the phenomenological NN potential for the long-range interaction. The agreement with the data but also the certainty in the data becomes less for higher energies, $\sqrt{s} \gtrsim 2.1$ GeV. This does not imply that the P-matrix approach has no validity. The agreement with the data can be improved if we allow ourselves more freedom in the residues and the poles in the P matrix. This will certainly become possible when there are more data at higher energies. Through the P matrix we then may learn the correct extrapolation of quark-quark interactions from few-quark to many-quark systems.

Improvements of the model and extension to negative-parity waves may come from the inclusion of the effects of orbitally and radially excited dibaryons. The d-wave and radially excited dibaryons probably will have influence also on baryon-baryon S waves, e.g., the $^3S_1$ and $^1S_0$ NN waves, for which the short-range interactions are very important. A glance at multiquark spectra[14] shows that it is almost unthinkable that one can account for all levels separately, except maybe for some which are very low lying. One therefore has to look for another approach which takes the collection of all levels into account. A possible way to continue is the combination of all quarks with a certain space symmetry. The occurrence of such configurations in specific nonstrange baryon-baryon waves has been calculated in Ref. 17.

We hope that an approach of the short-range interaction with the P matrix as described here does lead to a better understanding of the quark degrees of freedom in the short-range domain of hadronic interactions.

ACKNOWLEDGMENTS

The author would like to thank L. Heller for many discussions and valuable suggestions. He also acknowledges conversations with A. T. Aerts, D. C. Dodder, W. M. Kloet, A. S. Rinat, and R. R. Silbar. This research was supported by the U. S. Department of Energy.

APPENDIX

The main contributions in the phenomenological nucleon-nucleon potentials beyond 1 fm are the local central, tensor, and spin-orbit potentials. We assume that the effective quark-quark potential has the form

$$V_{qq}(\vec{r}) = \sum_{i,s} v_{is}^{(C)}(r) P_i P_s + \sum_i v_i^{(T)}(r) S_{qq} P_i + \sum_i v_i^{(SO)}(r) \vec{L}\cdot\vec{s} P_i ,$$

where P_i and P_S are isospin and spin projection operators for the two-quark system, S_{qq} is the tensor operator form [Eq. 8(a)], $\vec{s}$ is the spin of the two quarks, and $\vec{L}$ is the angular momentum between the two baryons. The potential for the NN system found from Eq. (7) yields

$$V_{NN}(\vec{r}) = \sum_{I,S} V_{IS}^{(C)}(r) P_I P_S + \sum_I V_I^{(T)}(r) S_{NN} P_I + \sum V_I^{(SO)}(r) \vec{L}\cdot\vec{S} P_I ,$$

where P_I, P_S, S_{NN}, and $\vec{S}$ are now two-nucleon operators. The relations between the NN and qq potentials are

$$\begin{bmatrix} V_{00}^{(C)} \\ V_{10}^{(C)} \\ V_{01}^{(C)} \\ V_{11}^{(C)} \end{bmatrix} = \frac{1}{18} \begin{bmatrix} 45 & 9 & 9 & 99 \\ 3 & 51 & 33 & 75 \\ 3 & 33 & 51 & 75 \\ 11 & 25 & 25 & 101 \end{bmatrix} \begin{bmatrix} v_{00}^{(C)} \\ v_{10}^{(C)} \\ v_{01}^{(C)} \\ v_{11}^{(C)} \end{bmatrix}$$

for the central potentials,

$$\begin{bmatrix} V_0^{(T)} \\ V_1^{(T)} \end{bmatrix} = \frac{1}{9} \begin{bmatrix} 21 & -12 \\ -4 & 13 \end{bmatrix} \begin{bmatrix} v_0^{(T)} \\ v_1^{(T)} \end{bmatrix}$$

for the tensor potentials, and

$$\begin{bmatrix} V_0^{(SO)} \\ V_1^{(SO)} \end{bmatrix} = \frac{1}{3} \begin{bmatrix} 6 & 3 \\ 1 & 8 \end{bmatrix} \begin{bmatrix} v_0^{(SO)} \\ v_1^{(SO)} \end{bmatrix}$$

for the spin-orbit potentials. Inverting these relations we find the quark-quark potentials v_{qq} from the NN potentials, for which we have used the phenomenological potentials from Ref. 11.

[1]R. A. Arndt, work presented at the Fifth International Symposium on Polarization Phenomena in Nuclear Physics, Santa Fe, New Mexico, 1980 (unpublished) and computer communication (interactive nucleon-nucleon program SAID).

[2]N. Hoshizaki, Prog. Theor. Phys. 61, 129 (1979); 60, 1796 (1978).

[3]K. Hashimoto, Y. Higuchi, and N. Hoshizaki, Prog. Theor. Phys. 64, 1678 (1980).

[4]J. Bolger *et al.*, Phys. Rev. Lett. 46, 167 (1981).

[5]W. M. Kloet and R. R. Silbar, Phys. Rev. Lett. 45, 970 (1980); W. M. Kloet, J. A. Tjon, and R. R. Silbar, Phys. Lett. 99B, 80 (1981).

[6]R. Bhandari, R. A. Arndt, L. D. Roper, and B. J. VerWest, Phys. Rev. Lett. 46, 1111 (1981).

[7]B. J. Edwards and G. H. Thomas, Phys. Rev. D 22, 2772 (1980).

[8]K. Kubodera, M. P. Locher, F. Myhrer, and A. W. Thomas, J. Phys. G. 6, 171 (1981).

[9]R. V. Reid, Ann. Phys. (N.Y.) 50, 411 (1968).

[10]M. M. Nagels, T. A. Rijken, and J. J. de Swart, Phys. Rev. D 12, 744 (1975); 17, 768 (1978).

[11]M. Lacombe *et al.*, Phys. Rev. D 12, 1495 (1975); Phys. Rev. C 21, 861 (1980).

[12]R. L. Jaffe, Phys. Rev. Lett. 38, 195 (1977).

[13]A. T. Aerts, P. J. Mulders, and J. J. de Swart, Phys. Rev. D 17, 260 (1978).

[14]P. J. Mulders, A. T. Aerts, and J. J. de Swart, Phys. Rev. Lett. 40, 1543 (1978); Phys. Rev. D 21, 2653 (1980).

[15]R. L. Jaffe and F. E. Low, Phys. Rev. D 19, 2105 (1979).

[16]V. Matveev and P. Sorba, Lett. Nuovo Cimento 20, 425 (1977).

[17]M. Harvey, Nucl. Phys. A352, 301 (1981); A352, 326 (1981).

[18]C. DeTar, Phys. Rev. D 17, 323 (1978); 19, 1451 (1979).

[19]Looking for q^6 states through poles in the P matrix as has been done in Ref. 15 is not possible because of the many inelastic channels which are open at energies where the lowest q^6 states are expected, $2.1-2.4$ GeV. The complete S matrix—and from the P matrix—cannot be recontructed from the data.

[20]We note that, using $r=2(\pi/b)^2\lambda^2$ for the residue of the pole in S wave $\pi\pi$ scattering (ϵ meson), the experimental residue, 0.32 GeV^2 (Ref. 15) agrees with the prediction for the $q^2\bar{q}^2$ bag state, $\lambda=0.643$ when $b\cong 5$ GeV^{-1}.

[21]H. Feshbach and E. Lomon, Ann. Phys. (N.Y.) 29, 19 (1964).

[22]C. Roiesnel, Phys. Rev. D 20, 1646 (1979).

[23]E. L. Lomon, in *Proceedings of the Workshop on Nuclear and Particle Physics at Energies Up to 31 GeV, Los Alamos, 1981,* edited by J. D. Bowman, L. S. Kisslinger, and R. R. Silbar (LASL, Los Alamos, 1981), p. 400.

[24]Note that $\lambda_\pm$ in general cannot be written as $\lambda_\pm=\cos\rho_\pm$ since $\lambda_\pm$ is not necessarily smaller than one. See, P. J. Mulders, Los Alamos National Laboratory Report No. LA-8879MS (unpublished).

[25]J. Arvieux and A. S. Rinat, Nucl. Phys. A350, 205 (1980); A. S. Rinat (private communication).

[26]Also in the $^3F_3$ NN wave the transition potential between NN and $N\Delta$ channels causes a resonant behavior which qualitatively explains the experimental phase shift.